

Elsevier Editorial System(tm) for Chemical Physics Letters
Manuscript Draft

Manuscript Number: CPLETT-10-2055R1

Title: Electronic transitions of iridium monoboride

Article Type: Regular Article

Section/Category: Gaseous Molecules

Corresponding Author: Dr. Allan Cheung, Ph.D

Corresponding Author's Institution: University of Hong Kong

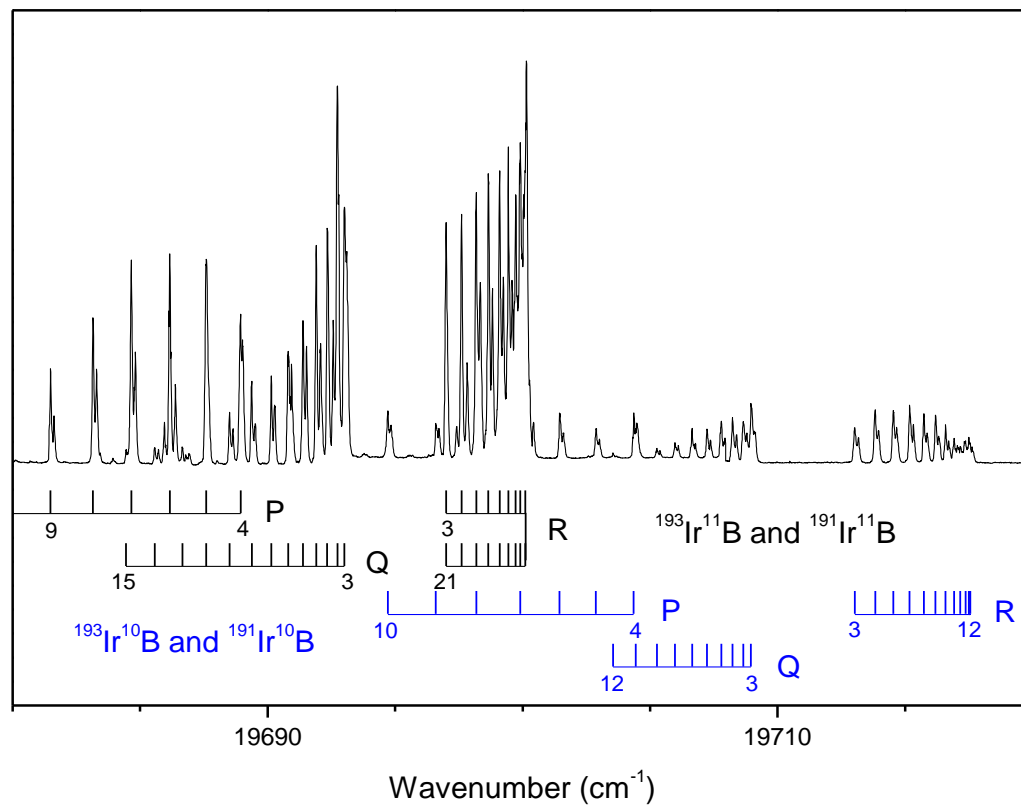
First Author: Hon F Pang, M.Sc.

Order of Authors: Hon F Pang, M.Sc.; Y W Ng, B.Sc.; Ye Xia, B.Sc.; Allan Cheung, Ph.D

Abstract: Electronic transitions spectrum of iridium monoboride in the spectral region between 400 and 545nm has been recorded and analyzed using laser vaporization/reaction free jet expansion source and laser induced fluorescence spectroscopy. Thirteen vibrational bands belonging to four electronic transitions, namely the [18.8] 3DEL3 - X3DEL3, [21.1] 3PHI4 - X3DEL3, [22.8] 3PHI3 - X3DEL3, and [22.4] 1PHI3 - a1DEL2 transitions, have been identified and rotationally analyzed. Spectra of all four isotopic molecules were observed.

Research Highlights:

- . New molecular transition bands of IrB
- . Four new electronic transitions have been observed and analyzed
- . Molecular constants of the upper and lower states were determined



Electronic transition spectrum of the (1, 0) band of the [18.8] $^3\Delta_3 - X^3\Delta_3$ system of IrB with all four isotopic molecules resolved

Electronic transitions of iridium monoboride

H.F. Pang, Y.W. Ng, Y. Xia and A.S-C. Cheung*

Department of Chemistry, The University of Hong Kong, Pokfulam Road, Hong Kong

Proposed running head: Electronic transitions of IrB

*Correspondence to:

Prof. A.S.C. Cheung

Department of Chemistry

The University of Hong Kong

Pokfulam Road

Hong Kong

Tel : (852) 2859 2155

Fax : (852) 2857 1586

Email : hrscsc@hku.hk

Text : 12

Tables : 2

Figures : 6

ABSTRACT

1 Electronic transitions spectrum of iridium monoboride in the spectral region between 400
2
3
4 and 545nm has been recorded and analyzed using laser vaporization/reaction free jet expansion
5
6
7 source and laser induced fluorescence spectroscopy. Thirteen vibrational bands belonging to four
8
9
10 electronic transitions, namely the [18.8] $^3\Delta_3 - X^3\Delta_3$, [21.1] $^3\Phi_4 - X^3\Delta_3$, [22.8] $^3\Phi_3 - X^3\Delta_3$, and
11
12
13 [22.4] $^1\Phi_3 - a^1\Delta_2$ transitions, have been identified and rotationally analyzed. Spectra of all four
14
15
16 isotopic molecules were observed.
17
18
19
20
21
22
23
24
25
26
27
28
29
30
31
32
33
34
35
36
37
38
39
40
41
42
43
44
45
46
47
48
49
50
51
52
53
54
55
56
57
58
59
60
61
62
63
64
65

I. INTRODUCTION

1
2 Metal borides (MB) are characterized by a great number of unique properties¹. Most of
3
4
5 the borides are refractory material with melting points above 2000K, high hardness and excellent
6
7
8 conductivity. Recently, there were reports on super-hardness properties of the rhenium boride
9
10
11 (ReB₂) bulk² and rhodium (RhB) and iridium (IrB) films³. The electrical conductivity of titanium
12
13
14 diboride (TiB₂) is known to be five times better than the titanium metal itself⁴. In addition,
15
16
17 magnesium diboride (MgB₂) was found to have superconductivity at 39K⁵. Despite of all these
18
19
20 important properties that have been found in MB, experimental study of MB molecules is very
21
22
23
24 limited.

25
26
27 Iridium containing species have long been an interesting research topic because of their
28
29
30 importance in iridium based alloys⁶ and also in catalytic processes involving the activation and
31
32
33 formation of carbon bonds (X = H, C, O, F etc.)^{7,8}. Spectroscopic properties of diatomic
34
35
36 molecules formed with Ir and main group elements of the 2p period have recently been
37
38
39 investigated, which include IrB⁹, IrC¹⁰, IrN¹¹, IrO¹², and IrF¹³. For iridium monoboride (IrB), our
40
41
42 group using laser induced fluorescence spectroscopy recorded vibrational bands of electronic
43
44
45 transition in the visible region between 545nm and 610nm, identified the ground X³Δ₃ state, and
46
47
48 reported the [16.5]³Π₂ – X³Δ₃ transition. Molecular parameters including hyperfine constants of
49
50
51 the ³Π₂ and ³Δ₃ states studied were determined.⁹
52
53
54
55
56
57
58
59
60
61
62
63
64
65

1 In this work, we report the analysis of thirteen vibrational bands belonging to four
2 electronic transitions recorded using the technique of laser vaporization reaction free jet
3 expansion and laser induced fluorescence (LIF) spectroscopy. Spectra of all the four isotopes:
4 $^{191}\text{Ir}^{10}\text{B}$, $^{193}\text{Ir}^{10}\text{B}$, $^{191}\text{Ir}^{11}\text{B}$ and $^{193}\text{Ir}^{11}\text{B}$ were resolved and studied.
5
6
7
8
9

10 II. EXPERIMENT

11 The experimental apparatus and detailed procedures for producing metal containing
12 molecules using laser vaporization/reaction free-jet expansion source and LIF spectroscopy have
13 been described in earlier publication.¹⁴ Only a brief description of the relevant experimental
14 conditions for obtaining IrB spectrum is given here. Frequency-doubled Nd:YAG laser pulses
15 with 5-6 mJ were focused onto the surface of an iridium rod to generate iridium atoms. A pulsed
16 valve was synchronized with appropriate time delay released gas mixture of 0.5% B_2H_6 in argon
17 to react with the iridium atoms for the production of IrB. A pulsed dye laser operated with
18 Coumarin dyes and pumped by a Nd:YAG laser with wavelength set to 355nm produced tunable
19 output in the visible region, which was used to excite the IrB molecules produced. The LIF
20 signal was collected by means of a lens system and detected by a photomultiplier tube (PMT).
21
22 The PMT output was fed to a fast oscilloscope for averaging and storage. The laser linewidth of
23 the tunable dye laser was about 0.07cm^{-1} . However, typical molecular linewidth obtained was
24 larger than 0.1cm^{-1} , which is likely to be due to unresolved hyperfine structure in the rotational
25 lines.
26
27
28
29
30
31
32
33
34
35
36
37
38
39
40
41
42
43
44
45
46
47
48
49
50
51
52
53
54
55
56
57
58
59
60
61
62
63
64
65

III. RESULTS AND DISCUSSION

A. Low Resolution Broadband Spectrum

Low resolution LIF spectrum of IrB in the spectral region between 400 to 545nm has been recorded. A broadband scan of the IrB spectrum is shown in Figure 1, which shows three transition systems. A total of 13 transition bands were recorded and analyzed. We were able to identify four electronic transitions, namely the [18.8] $^3\Delta_3 - X^3\Delta_3$, [21.1] $^3\Phi_4 - X^3\Delta_3$, [22.8] $^3\Phi_3 - X^3\Delta_3$, and [22.4] $^1\Phi_3 - a^1\Delta_2$ transitions. Except the [22.4] $^1\Phi_3 - a^1\Delta_2$ transition, all other three transitions originate from the ground $X^3\Delta_3$ state. As far as the least squares fitting of the molecular lines were concerned, for those lines originated from the ground $X^3\Delta_3$ state the rotational constant B was fixed at value determined earlier⁹. Figure 2 summarizes the electronic transitions identified and studied so far. Individual electronic transition observed is discussed in detail below. A list of the measured line positions of all the recorded transitions is deposited in the journal archive.

B. The [18.8] $^3\Delta_3 - X^3\Delta_3$ Transition

We have recorded three vibrational bands of this system: the (0, 0), (1, 0) and the (1, 1) bands. Figure 3 shows the (1, 0) band with all four isotopic molecules. The assignment of rotational structure was straight forward. The P, Q, and R branches are clearly resolved; from their respective first lines, namely P(4), Q(3) and R(3), we concluded that the upper state of this transition has an $\Omega = 3$ value. The intensity of the P and R branches is generally strong, which is

consistent with a $\Delta\Lambda = 0$ transition. The upper state is assigned to be ${}^3\Delta_3$ state. The observed line positions were fit to the following expression:

$$v = v_0 + B'J'(J'+1) - D'[J'(J'+1)]^2 - \{ B''J''(J''+1) - D''[J''(J''+1)]^2 \}, \quad (1)$$

where ' and '' refer to the usual rotation for the upper and the lower states, respectively. v_0 is the band origin, and B and D are the rotational and centrifugal distortion constants. Since only low J ($J < 12$), lines were measured. In the least squares fit, the centrifugal distortion constant was set to zero. Molecular constants obtained for the [18.8] ${}^3\Delta_3$ state are listed in Table 1. The $\Delta G_{1/2}$ value determined for the [18.8] ${}^3\Delta_3$ and the $X^3\Delta_3$ states are 931.88 and 909.64 cm^{-1} respectively for the most abundant ${}^{193}\text{Ir}^{11}\text{B}$ isotope.

C. The [21.1] ${}^3\Phi_4 - X^3\Delta_3$ Transition

Five vibrational bands of this electronic transition including the $(v, 0)$ with $v = 0 - 3$ and the $(0, 1)$ band were observed and analyzed. Fig. 4 shows the $(1, 0)$ band with well resolved P, Q and R branches. The first line of the respective branches are R(3), Q(4), and P(5), which established unambiguously the upper state has an $\Omega = 4$ value. The intensity of the R and Q branches are much larger than the P branch, which is consistent with a transition with $\Delta\Lambda = +1$. The upper state is, therefore, assigned as [21.1] ${}^3\Phi_4$ state. Least squares fit results of this transition is listed in Table 1. Again in this transition, all four isotopes were observed and analyzed. The $\Delta G_{1/2}$ of the $X^3\Delta_3$ state of the ${}^{193}\text{Ir}^{11}\text{B}$ isotope was determined to be 909.63 cm^{-1} , which agrees extremely well with the value determined from that of the [18.8] ${}^3\Delta_3 - X^3\Delta_3$ transition.

D. The [22.8] ${}^3\Phi_3 - X^3\Delta_3$ Transition

Three vibrational bands ($v, 0$) with $v = 0 - 2$ of this electronic transition were recorded and analyzed. Fig 5 depicts the (2, 0) band of this transition. The first line of the P, Q and the R branches are with J value equal to 4, 3 and 3 respectively, which indicate that the upper state is with an $\Omega = 3$ value. The intensity of the R and Q branches are stronger than the P branch, the upper state is, therefore, assigned as [22.8] $^3\Phi_3$ state. This transition is generally weaker than other transitions. We only obtained spectrum of the $^{191}\text{Ir}^{11}\text{B}$ and $^{193}\text{Ir}^{11}\text{B}$ molecules. Molecular constants obtained from fitting the rotational lines are listed in Table 1.

E. The [22.4] $^1\Phi_3 - a^1\Delta_2$ Transition

We recorded the (0, 0) and (1, 0) bands with heads at 22440 and 23128 cm^{-1} respectively. The (0, 0) band of this transition is shown in Fig 6. Assignment of rotational lines was straight forward. The first line of the branches are R(2), Q(3), and P(4), which indicates that the $\Omega' = 3$ and $\Omega'' = 2$. In addition, as shown in Fig. 6 the R and Q branches are stronger than the P branch, which is consistent with a $\Delta\Lambda = +1$ transition. The low resolution spectrum in Fig. 1 shows clearly that the two vibrational bands in this system are stronger in intensity than those other transitions originated from the same $X^3\Delta_3$ state. We have also recorded the resolved fluorescence spectrum of these bands. The vibrational separation of the lower state with $\Omega'' = 2$ is about 1018 $\pm 25 \text{ cm}^{-1}$, which is very different from the 909 cm^{-1} of the $X^3\Delta_3$ state. As far as the assignment of the lower state of this transition is concerned, we have considered the possibilities of $\Omega = 2$ of the $X^3\Delta$ state or of the $a^1\Delta$ state. We noticed that the spin-orbit of the Ir atom is very large and in the order of 2000 – 4000 cm^{-1} ¹⁵, IrB molecule formed would also be expected to have spin-orbit

components in the order of thousands of wavenumbers. Therefore, the $\Omega = 2$ component is expected to be located at much higher energy than the lowest $\Omega = 3$ component of the $X^3\Delta$ state and the population of the $\Omega = 2$ component should be very low when compares to the ground state. In addition, the rotational constant for the $X^3\Delta_3$ state is 0.5181 cm^{-1} , which is relatively larger than that of our determined $\Omega'' = 2$ level with a value of 0.5153 cm^{-1} . Based on the differences in transition intensity (the $a^1\Delta_2$ is a metastable state), vibrational separations and rotational constants mentioned above, we assigned the lower state of this transition to be the $a^1\Delta_2$ state. Consequently, the upper state is assigned as $^1\Phi_3$ state. The molecular constants obtained from the least squares fit of the observed lines for the two states are also listed in Table 1.

The four IrB isotopes are $^{191}\text{Ir}^{10}\text{B}$, $^{193}\text{Ir}^{11}\text{B}$, $^{191}\text{Ir}^{11}\text{B}$, and $^{193}\text{Ir}^{11}\text{B}$ and their relative natural abundance are respectively 0.15 0.25 0.59 and 1. Molecular parameters for the isotopic molecules are related by different powers of the mass dependence parameter $\rho = (\mu/\mu_i)$ when μ and μ_i are the reduced mass of an isotope and its heaviest isotope $^{193}\text{Ir}^{11}\text{B}$. The agreement between molecular constants of the four isotopes is excellent and, generally, with uncertainty in the range of one standard deviation of the molecular constants determined. It is because the vibrational separations of the excited states are to some extent shifted by unknown perturbation; it may not be useful or helpful to tabulate the equilibrium molecular constants.

F. Discussion

The ground of IrB as discussed in Ref. 9 is:



1 configurations with only one electron jump from the ground electronic configuration (Label A).
2
3
4 Many of the triplet states listed in the table are formed from molecular orbital (MO) with δ^3 or π^3
5
6
7 occupation, therefore, they are inverted states with the largest Ω value having the lowest energy.
8
9
10 It is well known that the iridium atom has large spin-orbit interaction and molecules formed from
11
12 iridium would generally have large spin-orbit splitting, and hence, the spin components with
13
14 different Ω values would be quite far apart. In such situation, the spin components should better
15
16
17 be described using Hund's case (c) coupling scheme¹⁶. In this work, using single electronic
18
19
20 configuration approach, the electronic transition observed can be considered as the promotion of
21
22
23 an electron from the ground state to the excited state with different electronic configurations. The
24
25
26 [16.5] $^3\Pi_2 - X^3\Delta_3$, [21.1] $^3\Phi_4 - X^3\Delta_3$ and [22.8] $^3\Phi_3 - X^3\Delta_3$ systems transition can be considered
27
28
29 as the promotion of an electron from the 2σ orbital (Label A) to the 2π orbital (Label D). The
30
31
32 difference between the band origins of the [21.1] $^3\Phi_4$ and [22.8] $^3\Phi_3$ states is about 1622 cm^{-1} , it is
33
34
35 reasonable that these states are the $\Omega = 3$ and $\Omega = 4$ components of the same inverted $^3\Phi_1$ state.
36
37
38 This assignment is consistent with the observation that the [22.8] $^3\Phi_3 - X^3\Delta_3$ transition is weaker
39
40
41 than the [21.1] $^3\Phi_4 - X^3\Delta_3$ transition because the $\Delta\Lambda = \Delta\Omega = +1$ should be the stronger sub-band
42
43
44 transition. In addition, the [22.4] $^1\Phi_3 - a^1\Delta_2$ transition would also arise from the promotion of an
45
46
47 electron from the 2σ (Label A) also 2π orbital (Label D). However, the [18.8] $^3\Delta_3 - X^3\Delta_3$
48
49
50 transition observed can be considered as the promotion of an electron from the 2σ orbital (Label
51
52
53 A) to the 3σ orbital (Label E). We have performed preliminary *ab initio* calculations on IrB and
54
55
56
57
58
59
60
61
62
63
64
65

1 the $a^1\Delta$ state was calculated to be about 1500 cm^{-1} above the $X^3\Delta$ state¹⁷. A detailed theoretical
2 computation with the level of theory down to individual spin-orbit components of each state will
3
4 be really useful to confirm our assignments here.
5
6

7 The aim of this work is to study the upper electronic states of the IrB molecule; this task is
8
9 getting more difficult because as we move up the energy scale, more and more states that could
10
11 only be identified with the Ω value. This is due, on the one hand, partially to the sizeable spin-
12
13 orbit interaction in the molecule and electronic states are practically in Hunds' case (c) coupling
14
15 scheme, it is difficult to assign any Λ value to these sub-states. On the other hand, the relatively
16
17 strong spectra of the Ir^{10}B isotopic molecule are widely separated from the Ir^{11}B , for instance,
18
19 the $v = 2$ level of the $[21.1]^3\Phi_3$ state the isotopic separation is over 28 cm^{-1} . Combining those
20
21 with the situation that the separation between vibrational levels is very often irregular, it is rather
22
23 difficult to link the spectra of isotopic molecules together. From our low resolution scan, we
24
25 have observed numerous bands that are comparable in intensity, but it is difficult to identify any
26
27 vibrational progressions. Similar excited state patterns have also been observed in the spectra of
28
29 iridium containing molecules such as IrC^{14} , IrN^{18} and also IrP^{19} .
30
31
32
33
34
35
36
37
38
39
40
41
42
43
44

45 **Acknowledgements**

46
47 The work described here was supported by a grant from the Research Grants Council of
48
49 the Hong Kong Special Administrative Region, China. (Project numbers HKU 701008).
50
51
52
53
54
55
56
57
58
59
60
61
62
63
64
65

References:

1. Y.G. Gogotsi and R.A. Andrievski, "Materials Science of Carbides, Nitrides, and Borides", *NATO Science Series* **Vol. 68**, Kluwer Academic Pub. 1999.
2. H. Chung, M.B. Weinberger, J.B. Levine, A. Kavner, J. Yang, S.H. Tolbert, and R.B. Kaner, *Science*, **316**, 436 (2007).
3. A. Latini, J.V. Rau, R. Teghil, A. Generosi, and V.R. Albertini, *App. Mater. Interfaces*, **2**, 581 (2010).
4. G. Will, *J. Solid State Chem.*, **177**, 628 (2004).
5. J. Nagamatsu, N. Nakagawa, T. Muranaka, Y. Zenitani, and J. Akimitsu, *Nature*, **410**, 63 (2001).
6. E.K. Ohrinu, R.D. Lanam, P. Panfilov, and H. Harada Eds, *Iridium-Proceedings of the international symposium*, The Minerals Metals and Materials Society (2000).
7. M.A. Ciriano, L.A. Oro and M.T. Camellini. *Organometallics*, **14**, (1995) 4764.
8. R. Jimenez-Catano and M.B. Hall. *Organometallics*, **15** (1996), 1889.
9. J. Ye, H.F. Pang, A. M-Y. Wong, J.W-H. Leung, and A. S-C. Cheung, *J. Chem. Phys.*, **128**, 154321 (2008).
10. A. J. Marr, M. E. Flores, and T.C. Steimle, *J. Chem. Phys.*, **104**, 8183 (1996).
11. T.C. Steimle, A.J. Marr, S.A. Beaton, and J.M. Brown, *J. Chem. Phys.*, **106**, 2073 (1997).
12. K. Jansson, and R. Scullman, *J. Mol. Spectrosc.*, **43**, 208 (1972).
13. A.G. Adam, A.D. Granger, L.E. Downie, D.W. Tokaryk and C. Linton, *Can. J. Phys.*, **87**, 557 (2009).
14. H.F. Pang and A. S-C Cheung, *Chem. Phys. Lett.*, **471** (2009) 194.
15. J.E. Sausonetti, W.C. Martin, and S.L. Young. *Handbook of basic atomic spectroscopic data (version 1.1.2) National Institute of Standard and Technology*, Gaithensburg. M.D. U.S.A. 2005.
16. G. Herzberg, *Spectra of Diatomic Molecules*, Van Nostrand, New York, 1950.

17. A. S-C. Cheung, H.F. Pang, Y. W. Ng, and Guanghui Chen, 65th OSU International Symposium on Molecular Spectroscopy, June 2010, Columbus, Ohio, USA. Paper WF02.

18. H.F. Pang and A. S-C. Cheung, *Chin. J. Chem. Phys.*, **22**, 157 (2009).

19. H.F. Pang, A. Liu, Y. Xia, and A. S-C. Cheung, *Chem. Phys. Lett.* **494**, 155 (2010).

1
2
3
4
5
6
7
8
9
10
11
12
13
14
15
16
17
18
19
20
21
22
23
24
25
26
27
28
29
30
31
32
33
34
35
36
37
38
39
40
41
42
43
44
45
46
47
48
49
50
51
52
53
54
55
56
57
58
59
60
61
62
63
64
65

Table legends:

1
2
3
4
5
6
7
8
9
10
11
12
13
14
15
16
17
18
19
20
21
22
23
24
25
26
27
28
29
30
31
32
33
34
35
36
37
38
39
40
41
42
43
44
45
46
47
48
49
50
51
52
53
54
55
56
57
58
59
60
61
62
63
64
65

Table 1 Molecular Constants for the [18.8]³Δ₃, [21.1]³Φ₄, [22.8]³Φ₃, [a+22.4]¹Φ₃, a¹Δ₂ and X³Δ₃ states of IrB

Table 2 Electronic configuration of low-lying excited states of IrB

Figure captions:

Figure 1. Broadband spectrum of IrB between 431 and 454 nm.

Figure 2. Observed electronic transition systems of IrB

Figure 3. (1, 0) band of the [18.8]³Δ₃ – X³Δ₃ transition of IrB

Figure 4. (1, 0) band of the [21.1]³Φ₄ – X³Δ₃ transition of IrB

Figure 5. (2, 0) band of the [22.8]³Φ₃ – X³Δ₃ transition of IrB

Figure 6. (0, 0) band of the [22.4]¹Φ₃ – a¹Δ₂ transition of IrB

Table 1. Molecular constants for the $[18.8]^3\Delta_3$, $[21.1]^3\Phi_4$, $[22.8]^3\Phi_3$, $[a + 22.4]^1\Phi_3$, $a^1\Delta_2$ and $X^3\Delta_3$ states of IrB (cm^{-1})

State	Parameter	$^{193}\text{Ir}^{11}\text{B}$	$^{191}\text{Ir}^{11}\text{B}$	$^{193}\text{Ir}^{10}\text{B}$	$^{191}\text{Ir}^{10}\text{B}$
[18.8] $^3\Delta_3$	T_1	19693.51(2)	19693.64(3)	19709.33(2)	19709.46(2)
	B_1	0.4805(2)	0.4806(3)	0.5300(3)	0.5301(2)
	T_0	18761.63(2)	18761.64(2)	18759.86(3)	18759.86(3)
[21.1] $^3\Phi_4$	B_0	0.5052(2)	0.5054(3)	0.5527(2)	0.5529(3)
	T_3	22554.49(4)	22554.57(3)	22580.81(3)	22580.92(3)
	B_3	0.4499(5)	0.4502(3)	0.4867(5)	0.4869(4)
	T_2	22158.00(6)	22158.26(6)	22186.30(6)	22186.57(5)
	B_2	0.4647(8)	0.4649(8)	0.5143(9)	0.5133(8)
	T_1	21650.29(5)	21650.33(5)	21661.64(8)	21661.71(8)
[22.8] $^3\Phi_3$	B_1	0.4687(4)	0.4693(5)	0.5153(8)	0.5154(8)
	T_0	21159.37(5)	21159.42(4)	21153.98(3)	21154.00(2)
	B_0	0.4855(7)	0.4856(6)	0.5321(3)	0.5323(3)
	T_2	24292.27(4)	24292.79(4)		
	B_2	0.4506(5)	0.4523(5)		
	T_1	23541.03(1)	23541.31(1)		
[a + 22.4] $^1\Phi_3$	B_1	0.4595(1)	0.4597(1)		
	T_0	22781.22(6)	22781.23(6)		
	B_0	0.4692(8)	0.4695(8)		
	T_1	a + 23122.17(3)	a + 23122.63(4)		
$a^1\Delta_2$	B_1	0.4668(6)	0.4683(8)		
	T_0	a + 22435.44 (2)	a + 22435.93(2)		
$X^3\Delta_3$	B_0	0.4609(1)	0.4612(2)		
	T_0	a	a		
	B_0	0.5153(2)	0.5156(3)		
	T_1	909.63(2)	909.92(2)		
	B_1	0.5140(3)	0.5142(3)		
	T_0	0.000	0.000	0.000	0.000
	B_0^*	0.51809	0.51839	0.56684	0.56713

Values given in parenthesis are one standard error in the last significant figure quoted

*Molecular constants from Ref. 9

1
2
3
4
5
6
7
8
9
10
11
12
13
14
15
16
17
18
19
20
21
22
23
24
25
26
27
28
29
30
31
32
33
34
35
36
37
38
39
40
41
42
43
44
45
46
47
48
49
50
51
52
53
54
55
56
57
58
59
60
61
62
63
64
65

Table 2. Electronic configurations of low-lying excited states of IrB

Label	Molecular Orbital Occupancies						Configuration	States
	1 σ	1 π	1 δ	2 σ	2 π	3 σ		
A	2	4	3	1			$\delta^3\sigma$	$X^3\Delta_i, a^1\Delta$
B	2	3	4	1			$\pi^3\sigma$	$^1\Pi, ^3\Pi_i$
C	2	4	2	2			δ^2	$^3\Sigma^-, ^1\Sigma^+, ^1\Gamma$
D	2	4	3		1		$\delta^3\pi$	$^3\Phi_i, ^3\Pi_i, ^1\Phi, ^1\Pi$
E	2	4	3			1	$\delta^3\sigma$	$^1\Delta, ^3\Delta_i$

1
2
3
4
5
6
7
8
9
10
11
12
13
14
15
16
17
18
19
20
21
22
23
24
25
26
27
28
29
30
31
32
33
34
35
36
37
38
39
40
41
42
43
44
45
46
47
48
49
50
51
52
53
54
55
56
57
58
59
60
61
62
63
64
65

Figure 1

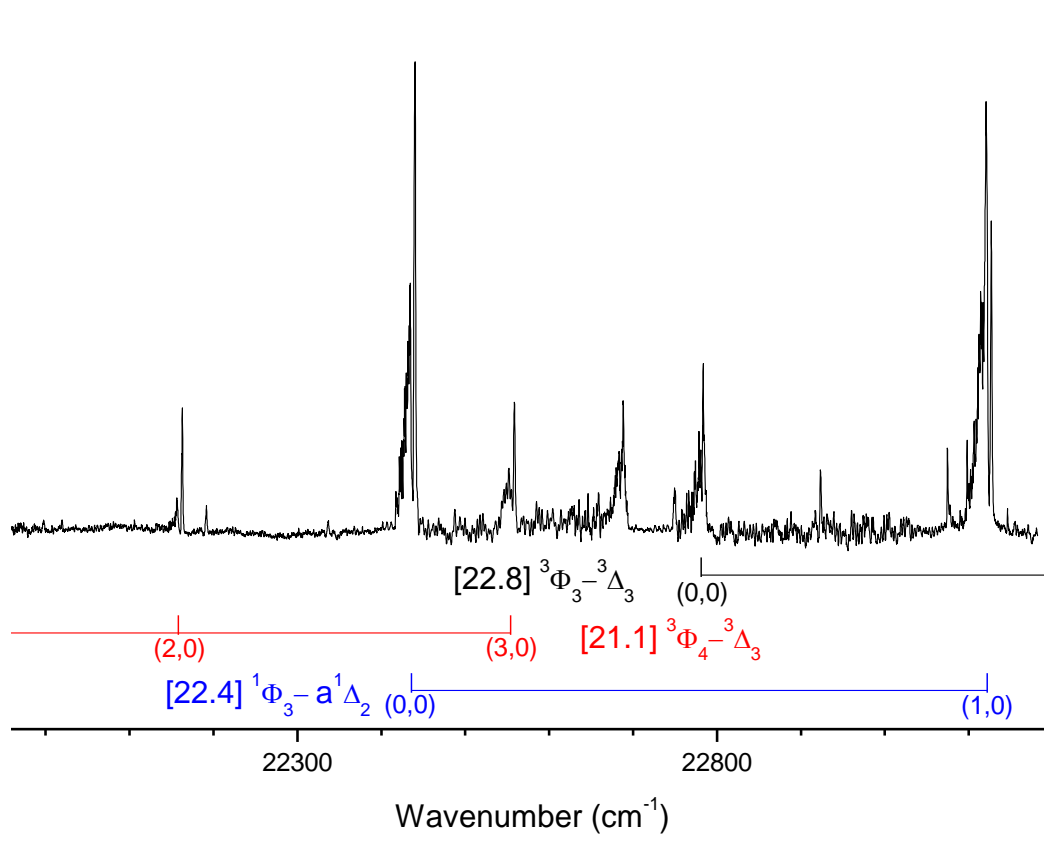


Figure 2

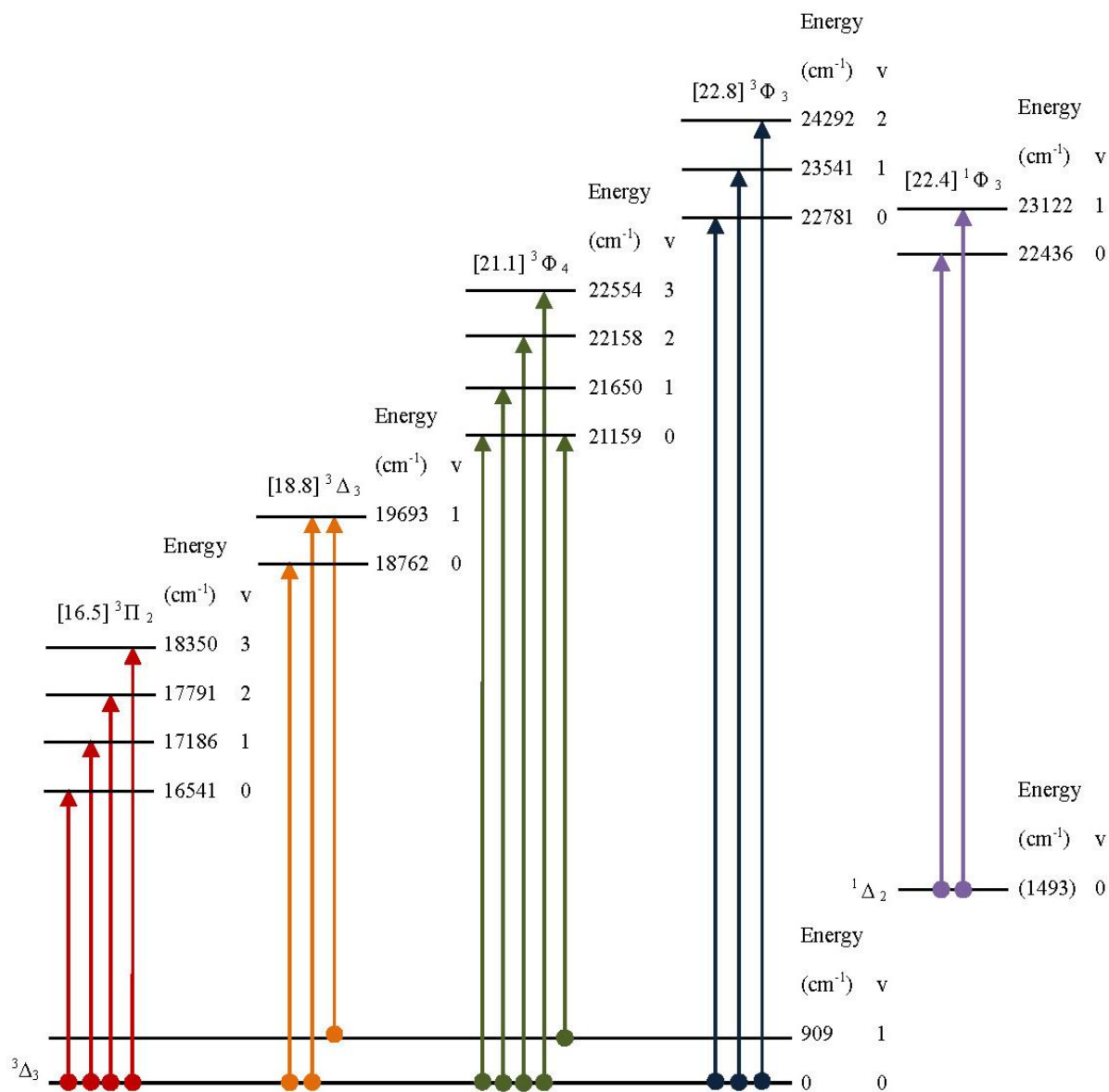


Figure 3

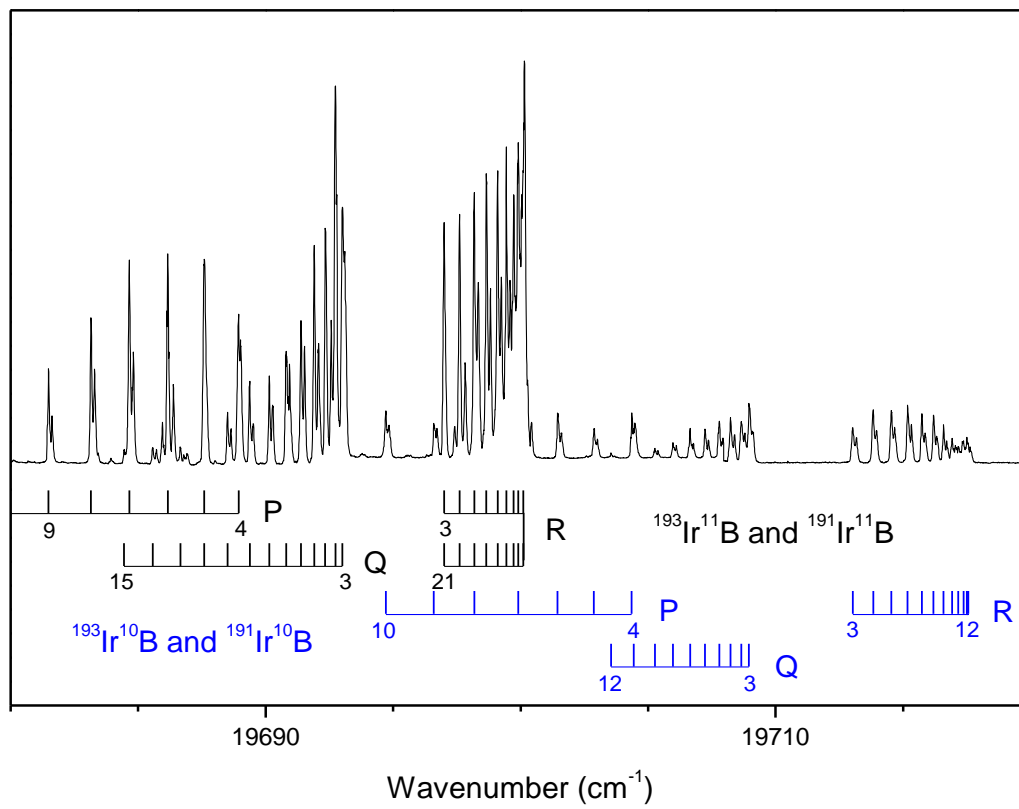


Figure 4

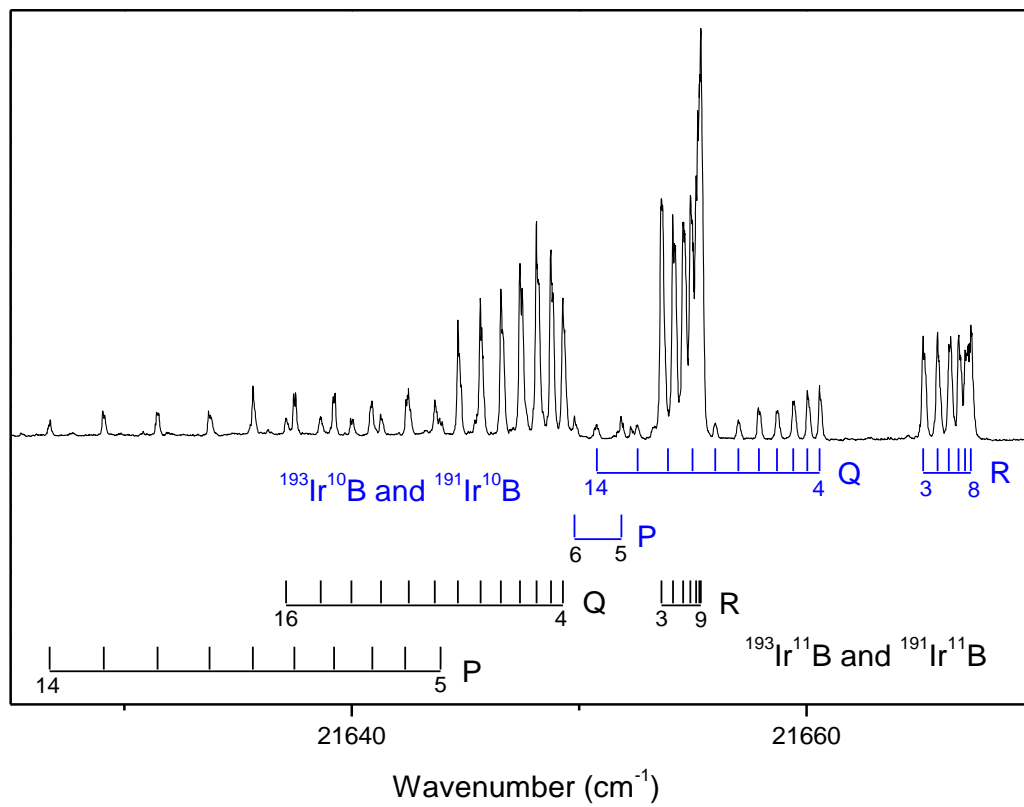


Figure 5

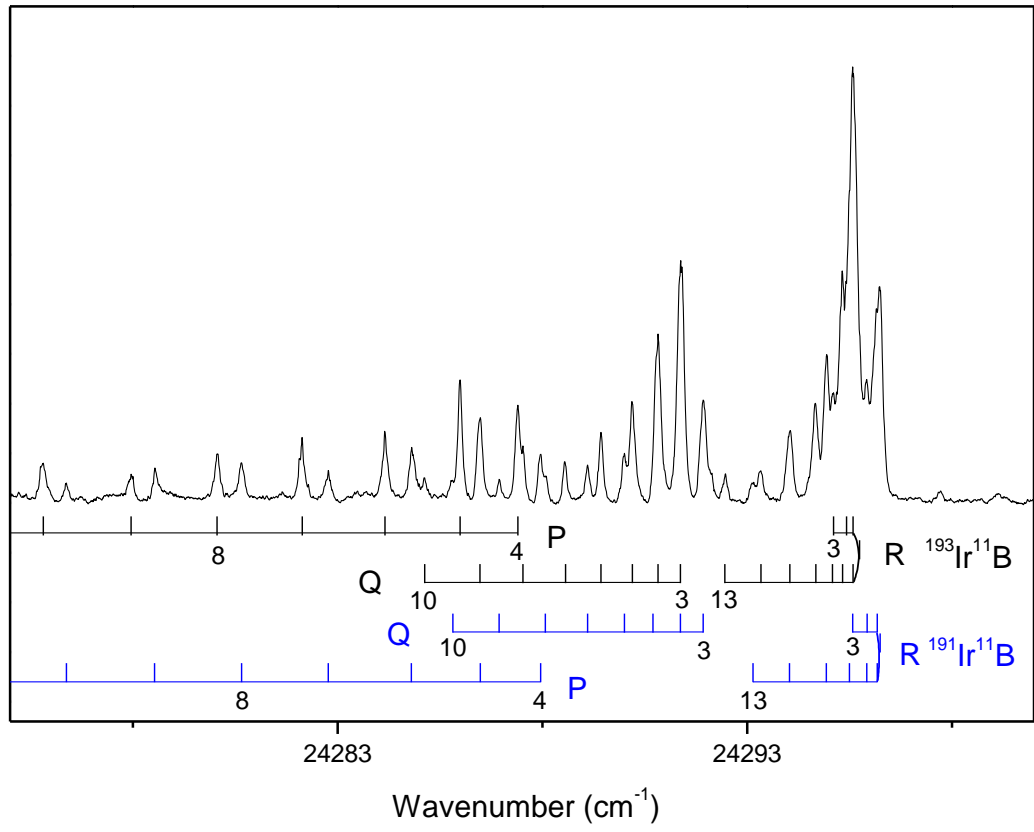
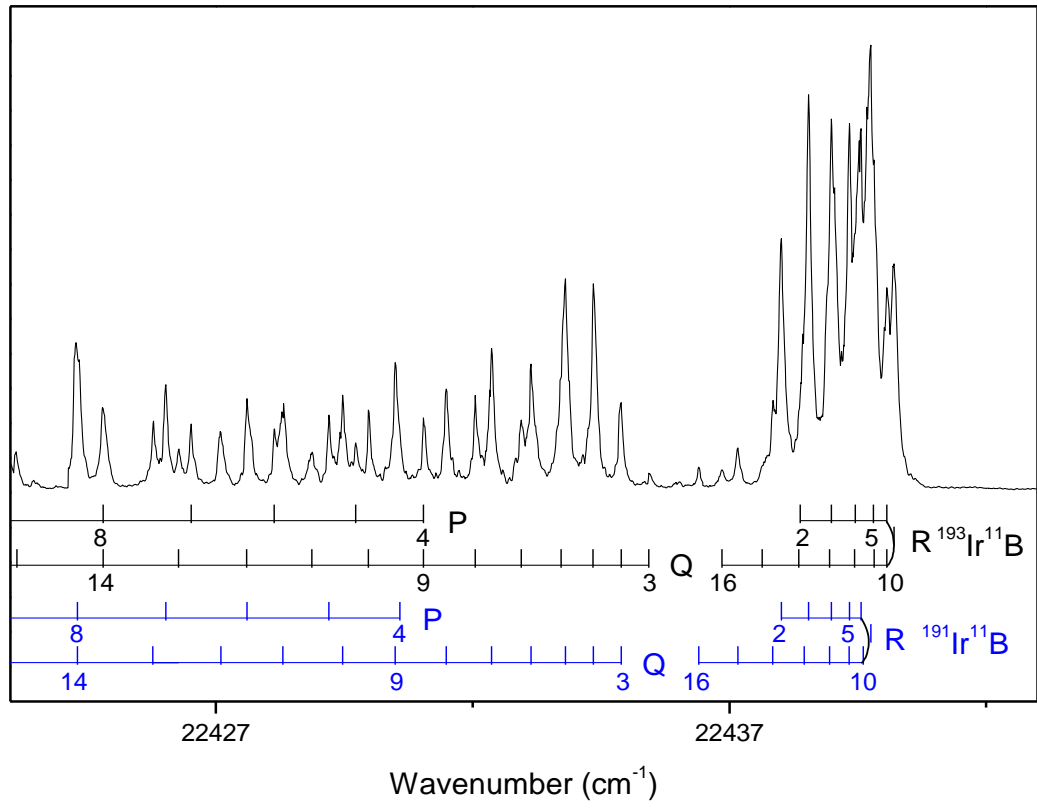


Figure 6



$^{191}\text{Ir}^{10}\text{B}$ and $^{193}\text{Ir}^{10}\text{B}$ Assigned rotational lines of the $[18.8] \ ^3\Delta_3 - X \ ^3\Delta_3$ transition

(0,0)			
J	P	Q	R
3		18759.76	18764.10
4	18755.10	18759.74	18765.06
5	18753.77	18759.41	18765.96
6	18752.48	18759.26	18766.96
7	18751.29*	18759.02	18767.94
8	18750.02	18758.74	18768.97
9	18748.69	18758.47	18769.78
10	18747.36	18758.20	18770.63
11	18746.01		18771.35
12	18744.47		18772.02
13	18742.87		18772.78*
14	18741.23		18773.42*
15			18774.09*
16			18774.69*

 $^{191}\text{Ir}^{11}\text{B}$ and $^{193}\text{Ir}^{11}\text{B}$ Assigned rotational lines of the $[18.8] \ ^3\Delta_3 - X \ ^3\Delta_3$ transition

(0,0)			
J	P	Q	R
3		18761.48	18765.41
4	18757.48	18761.40	18766.31
5	18756.24	18761.29	18767.20
6	18754.94	18761.14	18768.16
7	18753.66	18760.96	18769.06
8	18752.48	18760.75	18769.92
9	18751.29*	18760.52	18770.70
10	18750.07	18760.23	18771.43
11	18748.80		18772.14
12	18747.52		18772.78*
13	18746.22		18773.42*
14	18744.79		18774.09*
15	18743.32		18774.69*
16	18741.78		18775.21

* indicate overlapped with another line

$^{191}\text{Ir}^{10}\text{B}$ Assigned rotational lines of the $[18.8] \ ^3\Delta_3 - \text{X} \ ^3\Delta_3$ transition

(1,0)

J	P	Q	R
3		19709.10	19713.17
4	19704.49	19708.80	19713.96
5	19703.02	19708.39	19714.67
6	19701.61	19707.94	19715.34
7	19700.05	19707.37	19715.87
8	19698.35	19706.77	19716.33
9	19696.74	19706.11	19716.71
10	19694.84	19705.40	19717.06
11		19704.52	19717.32
12			19717.55
13			19717.67*
14			19717.67*

 $^{193}\text{Ir}^{10}\text{B}$ Assigned rotational lines of the $[18.8] \ ^3\Delta_3 - \text{X} \ ^3\Delta_3$ transition

(1,0)

J	P	Q	R
3		19708.96	19713.03
4	19704.36	19708.65	19713.83
5	19702.88	19708.23	19714.54
6	19701.45	19707.80	19715.18
7	19699.91	19707.24	19715.74
8	19698.18	19706.65	19716.20
9	19696.59	19705.97	19716.59
10	19694.72	19705.27	19716.93
11		19704.43	19717.17
12		19703.55	19717.37
13			19717.50*
14			19717.55
15			19717.50*

* indicate overlapped with another line

$^{191}\text{Ir}^{11}\text{B}$ Assigned rotational lines of the $[18.8] \ ^3\Delta_3 - X \ ^3\Delta_3$ transition

(1,0)

J	P	Q	R
3		19693.11	19697.00
4		19692.79	19697.82*
5	19687.60*	19692.57	19698.35*
6	19686.38	19692.08	19698.82*
7	19684.82	19691.53	19699.25*
8	19683.29	19690.94	19699.59*
9	19681.62	19690.28	19699.91*
10	19679.83	19689.52	19700.10
11	19677.98	19688.64	19700.15*
12	19676.16	19687.60*	19700.15*
13	19674.17*	19686.79	19700.15*
14	19672.34	19685.72	19700.05
15	19670.07	19684.65	19699.91*
16	19668.06		19699.59*
17	19665.68		19699.25*
18	19663.41		19698.82*
19			19698.35*
20			19697.82*

* indicate overlapped with another line

$^{193}\text{Ir}^{11}\text{B}$ Assigned rotational lines of the $[18.8] \ ^3\Delta_3 - X \ ^3\Delta_3$ transition

(1,0)

J	P	Q	R
3		19693.01	19697.00*
4	19688.94	19692.74	19697.60*
5	19687.60*	19692.34	19698.18*
6	19686.16	19691.91	19698.65*
7	19684.65	19691.39	19699.10*
8	19683.15	19690.81	19699.44*
9	19681.48	19690.15	19699.73*
10	19679.68	19689.38	19699.91*
11	19677.86	19688.51	19700.10*
12	19676.04	19687.60*	19700.15
13	19674.17*	19686.66	19700.10*
14	19672.05	19685.57	19699.91*
15	19669.94	19684.44	19699.73*
16	19667.94		19699.44*
17	19665.55		19699.10*
18	19663.29		19698.65*
19			19698.18*
20			19697.60*
21			19697.00*

* indicate overlapped with another line

$^{191}\text{Ir}^{11}\text{B}$ and $^{193}\text{Ir}^{11}\text{B}$ Assigned rotational lines of the $[18.8] \ ^3\Delta_3 - \text{X} \ ^3\Delta_3$ transition

(1,1)

J	P	Q	R
3		18783.58	18787.35
4	18779.26	18783.36	18787.99
5	18777.93	18783.00	18788.57
6	18776.57	18782.54	18789.07
7		18782.08	18789.53
8			18789.96

* indicate overlapped with another line

$^{191}\text{Ir}^{10}\text{B}$ Assigned rotational lines of the $[21.1] \ ^3\Phi_4 - X^3\Delta_3$ transition

(0,0)

J	P	Q	R
3			21157.96*
4		21153.34*	21158.57*
5	21147.58*	21152.92*	21159.28
6	21146.16*	21152.40*	21159.98
7	21144.67*	21152.04*	21160.61*
8	21143.05	21151.46*	21161.09*
9	21141.23	21150.92*	21161.52*
10		21150.29*	21161.87*
11			21162.15*
12			21162.36
13			21162.54

 $^{193}\text{Ir}^{10}\text{B}$ Assigned rotational lines of the $[21.1] \ ^3\Phi_4 - X^3\Delta_3$ transition

(0,0)

J	P	Q	R
3			21157.96*
4		21153.34*	21158.57*
5	21147.58*	21152.92*	21159.20
6	21146.16*	21152.40*	21159.91
7	21144.67*	21152.04*	21160.61*
8	21142.97	21151.46*	21161.09*
9	21141.11	21150.92*	21161.52*
10		21150.29*	21161.87*
11			21162.15*
12			21162.36*
13			21162.51

* indicate overlapped with another line

$^{191}\text{Ir}^{11}\text{B}$ Assigned rotational lines of the $[21.1] \ ^3\Phi_4 - X^3\Delta_3$ transition

(0,0)

J	P	Q	R
3			21163.08
4		21158.78*	21163.75*
5	21153.34	21158.43*	21164.36
6	21152.19	21157.96*	21164.93*
7	21150.69	21157.53	21165.45
8	21149.32	21156.96*	21165.86
9	21147.84*	21156.39	21166.19*
10		21155.74	21166.49*
11			21166.77*
12			
13			

 $^{193}\text{Ir}^{11}\text{B}$ Assigned rotational lines of the $[21.1] \ ^3\Phi_4 - X^3\Delta_3$ transition

(0,0)

J	P	Q	R
3			21163.10
4		21158.78*	21163.75*
5	21153.33	21158.43*	21164.17
6	21152.04	21157.96*	21164.93*
7	21150.61	21157.49	21165.41
8	21149.23	21156.96*	21165.81
9	21147.84*	21156.32	21166.19*
10		21155.64	21166.49*
11			21166.77*
12			
13			

* indicate overlapped with another line

$^{191}\text{Ir}^{11}\text{B}$ Assigned rotational lines of the $[21.1] \ ^3\Phi_4 - X \ ^3\Delta_3$ transition

(0,1)			
J	P	Q	R
3			20253.09
4		20249.08*	20253.81
5	20243.66	20248.72	20254.47
6	20242.35	20248.32	20255.06
7	20241.00	20247.84	20255.63
8	20239.64	20247.33	20256.09
9	20238.19	20246.70	20256.54
10	20236.69		20256.92
11			20257.27
12			20257.54*
13			

 $^{193}\text{Ir}^{11}\text{B}$ Assigned rotational lines of the $[21.1] \ ^3\Phi_4 - X \ ^3\Delta_3$ transition

(0,1)			
J	P	Q	R
3			20253.35
4		20249.08*	20254.05
5	20243.93	20248.78	20254.69
6	20242.60	20248.45	20255.32
7	20241.26	20248.04	20255.85
8	20239.88	20247.60	20256.36
9	20238.44	20247.07	20256.80
10	20236.95		20257.19
11			20257.54*
12			20257.77
13			20258.02
14			20258.25
15			20258.32

* indicate overlapped with another line

$^{191}\text{Ir}^{10}\text{B}$ Assigned rotational lines of the $[21.1] \ ^3\Phi_4 - X \ ^3\Delta_3$ transition

(1,0)

J	P	Q	R
3			21665.19
4		21660.65	21665.82
5		21660.10	21666.34
6		21659.45	21666.77
7	21651.92	21658.74	
8	21649.88	21657.95	
9		21657.06	

 $^{193}\text{Ir}^{10}\text{B}$ Assigned rotational lines of the $[21.1] \ ^3\Phi_4 - X \ ^3\Delta_3$ transition

(1,0)

J	P	Q	R
3			21665.13
4		21660.57	21665.76
5		21660.03	21666.26
6		21659.40	21666.69
7	21651.85	21658.67	
8	21649.79	21657.88	
9		21657.00	

* indicate overlapped with another line

$^{191}\text{Ir}^{11}\text{B}$ Assigned rotational lines of the $[21.1] \ ^3\Phi_4 - X \ ^3\Delta_3$ transition

(1,0)

J	P	Q	R
3			21653.65
4		21649.34	21654.20
5	21643.87	21648.85*	21654.65
6	21642.50*	21648.21*	21654.98*
7	21640.89	21647.50*	21655.21
8	21639.27*	21646.64	21655.31
9	21637.53*	21645.71*	21655.35*
10	21635.65*	21644.73	
11	21633.79	21643.65*	
12	21631.52	21642.50*	
13	21629.14	21641.36	
14	21626.74	21640.06*	
15	21624.42*		

 $^{193}\text{Ir}^{11}\text{B}$ Assigned rotational lines of the $[21.1] \ ^3\Phi_4 - X \ ^3\Delta_3$ transition

(1,0)

J	P	Q	R
3			21653.62
4		21649.28	21654.12
5	21643.97	21648.85*	21654.60
6	21642.50*	21648.21*	21654.98*
7	21640.90	21647.50*	21655.14
8	21639.27*	21646.55	21655.29
9	21637.53*	21645.71*	21655.35*
10	21635.65*	21644.67	
11	21633.70	21643.65*	
12	21631.51	21642.50*	
13	21629.13	21641.27	
14	21626.74*	21640.06*	
15	21624.42*	21638.64	
16	21621.92	21637.11	

* indicate overlapped with another line

$^{191}\text{Ir}^{10}\text{B}$ Assigned rotational lines of the $[21.1] \ ^3\Phi_4 - X \ ^3\Delta_3$ transition

(2,0)

J	P	Q	R
3			22189.97
4		22185.55	22190.51
5	22179.97	22185.00	22190.98
6	22178.28*	22184.36	22191.35*
7	22176.37*	22183.58	22191.61*
8	22174.51	22182.69	
9	22172.62	22181.74	
10	22170.11	22180.70	
11			
12		22178.28*	

 $^{193}\text{Ir}^{10}\text{B}$ Assigned rotational lines of the $[21.1] \ ^3\Phi_4 - X \ ^3\Delta_3$ transition

(2,0)

J	P	Q	R
3			22189.77
4		22185.36	22190.33
5	22179.28	22184.80	22190.77
6	22177.89*	22184.16	22191.10
7	22176.37*	22183.37	22191.35*
8	22174.21	22182.48	22191.61*
9	22171.99	22181.51	
10	22170.04	22180.58	
11			
12		22177.89*	

* indicate overlapped with another line

$^{191}\text{Ir}^{11}\text{B}$ Assigned rotational lines of the $[21.1] \ ^3\Phi_4 - \text{X} \ ^3\Delta_3$ transition

(2,0)

J	P	Q	R
3			22161.45
4		22157.32	22161.93
5	22151.73	22156.73	22162.35*
6	22150.18	22156.02	22162.57
7	22148.54	22155.21	22162.83*
8	22147.00	22154.30	22162.83*
9	22145.05	22153.28	
10	22143.17	22152.17	
11	22141.16	22151.00	
12	22138.96	22149.74	

 $^{193}\text{Ir}^{11}\text{B}$ Assigned rotational lines of the $[21.1] \ ^3\Phi_4 - \text{X} \ ^3\Delta_3$ transition

(2,0)

J	P	Q	R
3			22161.21
4		22157.07	22161.71
5	22151.50	22156.47	22162.09
6	22149.96	22155.77	22162.35*
7	22148.33	22154.98	
8	22146.63	22154.05	
9	22144.85	22153.06	
10	22142.95	22152.94	
11	22140.93	22150.78	
12	22138.72	22149.52	

* indicate overlapped with another line

$^{191}\text{Ir}^{10}\text{B}$ Assigned rotational lines of the $[21.1] \ ^3\Phi_4 - \text{X} \ ^3\Delta_3$ transition

(3,0)

J	P	Q	R
3			22583.90*
4		22579.34	22584.21*
5	22573.66*	22578.55	22584.28*
6	22571.28	22577.63	22584.28*
7	22569.21	22576.51	22584.21*
8	22567.05	22575.16	22583.90*
9	22564.85	22573.66*	
10	22562.35	22572.05	
11		22570.32	
12		22568.51	

 $^{193}\text{Ir}^{10}\text{B}$ Assigned rotational lines of the $[21.1] \ ^3\Phi_4 - \text{X} \ ^3\Delta_3$ transition

(3,0)

J	P	Q	R
3			22583.64
4		22579.21	22584.09*
5	22573.53*	22578.45	22584.21*
6	22571.18	22577.52	22584.28*
7	22569.10	22576.39	22584.09*
8	22566.95	22575.03	22583.90*
9	22564.74	22573.53*	
10	22562.33	22571.95	
11		22570.21	

* indicate overlapped with another line

$^{191}\text{Ir}^{11}\text{B}$ Assigned rotational lines of the $[21.1] \ ^3\Phi_4 - X \ ^3\Delta_3$ transition

(3,0)

J	P	Q	R
3			22557.29*
4		22553.28	22557.77*
5	22548.06	22552.53	22557.99*
6	22546.29	22551.68	22557.99*
7	22544.50	22550.68	22557.99*
8	22542.62	22549.57	22557.64*
9	22540.60	22548.34	22557.29*
10		22546.97	22555.77*
11		22545.50	22554.74
12		22543.93	
13		22542.24	

 $^{193}\text{Ir}^{11}\text{B}$ Assigned rotational lines of the $[21.1] \ ^3\Phi_4 - X \ ^3\Delta_3$ transition

(3,0)

J	P	Q	R
3			22557.15
4		22553.14	22557.64*
5	22547.84	22552.40	22557.99*
6	22546.17	22551.55	22557.99*
7	22544.37	22550.55	22557.99*
8	22542.51	22549.44	22557.76
9	22540.37	22548.21	
10		22546.84	
11		22545.36	
12		22543.79	
13		22542.06	

* indicate overlapped with another line

$^{191}\text{Ir}^{11}\text{B}$ and $^{193}\text{Ir}^{11}\text{B}$

Assigned rotational lines of the [22.8] $^3\Phi_3 - X^3\Delta_3$ transition

(0,0)

J	P	Q	R
3		22780.60	22784.48
4	22776.58	22780.14	22784.98
5	22775.13	22779.62	22785.46
6	22773.63	22779.01	22785.79
7	22772.05		22785.93
8	22770.24		

* indicate overlapped with another line

$^{191}\text{Ir}^{11}\text{B}$ Assigned rotational lines of the $[22.8] \ ^3\Phi_3 - \text{X} \ ^3\Delta_3$ transition

(1,0)

J	P	Q	R
3		23540.61	23544.35
4	23536.49	23540.11	23544.81
5	23534.94*	23539.50	23545.06*
6	23533.31	23538.79	23545.31*
7	23531.62	23537.95	23545.39
8	23529.78	23537.06	23545.31*
9	23527.76	23536.04	23545.22
10	23525.60	23534.94*	23545.06*
11	23523.41		23544.51
12	23521.10		23544.08
13	23518.63		23543.56
14	23516.14		23542.81
15			23541.94

 $^{193}\text{Ir}^{11}\text{B}$ Assigned rotational lines of the $[22.8] \ ^3\Phi_3 - \text{X} \ ^3\Delta_3$ transition

(1,0)

J	P	Q	R
3		23540.31	23544.08
4	23536.20	23539.83	23544.51*
5	23534.66	23539.22	23544.81
6	23533.07	23538.51	23545.06*
7	23531.34	23537.69	23545.12*
8	23529.52	23536.80	23545.12*
9	23527.50	23535.76	23545.06*
10	23525.32		23544.73
11	23523.16		23544.35
12	23520.82		23543.88
13	23518.41		23543.26
14			23542.52
15			23541.65

* indicate overlapped with another line

$^{191}\text{Ir}^{11}\text{B}$ Assigned rotational lines of the $[22.8] \ ^3\Phi_3 - \text{X} \ ^3\Delta_3$ transition

(2,0)

J	P	Q	R
3		24291.92	24295.57
4	24287.95	24291.37	24295.90
5	24286.48	24290.70	24296.22*
6	24284.80	24290.00	24296.22*
7	24282.77	24289.10	24296.22*
8	24280.65	24288.07	24296.17
9	24278.53		24295.92
10	24276.38		24295.49
11	24274.11		24294.83
12	24271.73		
13	24269.02		

 $^{193}\text{Ir}^{11}\text{B}$ Assigned rotational lines of the $[22.8] \ ^3\Phi_3 - \text{X} \ ^3\Delta_3$ transition

(2,0)

J	P	Q	R
3		24291.34	24295.10*
4	24287.40	24290.82	24295.42
5	24285.99	24290.19	24295.58*
6	24284.15	24289.43	24295.74
7	24282.13	24288.54	24295.58*
8	24280.05		24295.49
9	24277.95		24295.10*
10	24275.81		24294.67
11	24273.58		24294.04
12	24271.16		24293.33
13	24268.27		24292.45

* indicate overlapped with another line

$^{191}\text{Ir}^{11}\text{B}$ Assigned rotational lines of the [22.4] $^1\Phi_3 - a^1\Delta_2$ transition

(0,0)

J	P	Q	R
2			22438.38
3		22435.46	22438.98
4	22431.05*	22434.89	22439.46
5	22429.72	22434.27	22439.80
6	22428.13	22433.73	22440.07
7	22426.52	22432.95	22440.21*
8		22432.05	22440.21*
9		22431.05*	22440.21*
10		22429.97	22440.07*
11			
12			
13			
14			22438.39
15			22437.73
16			22436.86

* indicate overlapped with another line

$^{193}\text{Ir}^{11}\text{B}$ Assigned rotational lines of the [22.4] $^1\Phi_3 - a^1\Delta_2$ transition

(0,0)

J	P	Q	R
2			22438.01
3			22438.54
4	22430.58	22434.35	22438.98
5	22429.20	22433.81	22439.34
6	22427.60	22433.14	22439.56
7	22426.03	22432.37	22439.75*
8		22431.49	22439.75*
9		22430.49	22439.70
10		22429.47	22439.52
11			22439.28
12			22438.90
13			22438.44
14			22437.85
15			22437.17
16			22436.41

* indicate overlapped with another line

$^{191}\text{Ir}^{11}\text{B}$ Assigned rotational lines of the [22.4] $^1\Phi_3 - a^1\Delta_2$ transition

(1,0)

J	P	Q	R
2			23125.28
3		23121.95	23125.89*
4	23118.01	23121.55*	23126.39
5	23116.53	23121.17*	23127.00
6	23114.98	23120.57	23127.26
7	23113.45	23120.01	23127.41
8	23111.74	23119.21	
9		23118.41	

 $^{193}\text{Ir}^{11}\text{B}$ Assigned rotational lines of the [22.4] $^1\Phi_3 - a^1\Delta_2$ transition

(1,0)

J	P	Q	R
2			23124.83
3		23121.55*	23125.42
4	23117.52	23121.17*	23125.89*
5	23116.00	23120.70	23126.34
6	23114.43	23120.12	23126.70
7	23112.91	23119.48	23126.77
8	23111.22	23118.75	
9	23109.46	23117.89	
10	23107.54		

* indicate overlapped with another line